Mutations in ionotropic AMPA receptor 3 alter channel properties and are associated with moderate cognitive impairment in humans

Ye Wu[a,b], Amy C. Arai[c], Gavin Rumbaugh[d,e], Anand K. Srivastava[f], Gillian Turner[g], Takashi Hayashi[d,e], Erika Suzuki[c], Yuwu Jiang[a,b], Lilei Zhang[a], Jayson Rodriguez[f], Jackie Boyle[g], Patrick Tarpey[h], F. Lucy Raymond[i], Joke Nevelsteen[j], Guy Froyen[j], Mike Stratton[h], Andy Futreal[h], Jozef Gecz[k], Roger Stevenson[f], Charles E. Schwartz[f], David Valle[a], Richard L. Huganir[d,e], and Tao Wang[a,l]

[a]Institute of Genetic Medicine and Department of Pediatrics, [d]Department of Neuroscience, and [e]Howard Hughes Medical Institute, Johns Hopkins University School of Medicine, Baltimore, MD 21205; [c]Department of Pharmacology, Southern Illinois University School of Medicine, Springfield, IL 62794; [f]Greenwood Genetic Center, Greenwood, SC 29646; [g]Hunter Genetics and Genetics of Learning Disability (GOLD) Service, University of Newcastle, Callaghan NSW 2308, Australia; [h]Wellcome Trust Sanger Institute, Wellcome Trust Genome Campus, Cambridge CB10 1SA, United Kingdom; [i]Department of Medical Genetics, Cambridge Institute of Medical Research, University of Cambridge, Cambridge CB2 2XY, United Kingdom; [j]Human Genome Laboratory, Department of Human Genetics, Vlaams Instituut voor Biotechnologie, University of Leuven, 3000 Leuven, Belgium; [k]Department of Genetic Medicine, Women's and Children's Hospital, and Departments of Pediatrics and Molecular Biosciences, University of Adelaide, Adelaide SA 5005, Australia; and [b]Department of Pediatrics, Beijing University First Hospital, Beijing 100034, People's Republic of China

Communicated by C. Thomas Caskey, University of Texas–Houston Health Science Center, Houston, TX, September 14, 2007 (received for review May 16, 2007)

Ionotropic α-amino-3-hydroxy-5-methyl-4-isoxazolepropionic acid (AMPA) receptors (iGluRs) mediate the majority of excitatory synaptic transmission in the CNS and are essential for the induction and maintenance of long-term potentiation and long-term depression, two cellular models of learning and memory. We identified a genomic deletion (0.4 Mb) involving the entire *GRIA3* (encoding iGluR3) by using an X-array comparative genomic hybridization (CGH) and four missense variants (G833R, M706T, R631S, and R450Q) in functional domains of iGluR3 by sequencing 400 males with X-linked mental retardation (XLMR). Three variants were found in males with moderate MR and were absent in 500 control males. Expression studies in HEK293 cells showed that G833R resulted in a 78% reduction of iGluR3 due to protein misfolding. Whole-cell recording studies of iGluR3 homomers in HEK293 cells revealed that neither iGluR3-M706T (S2 domain) nor iGluR3-R631S (near channel core) had substantial channel function, whereas R450Q (S1 domain) was associated with accelerated receptor desensitization. When forming heteromeric receptors with iGluR2 in HEK293 cells, all four iGluR3 variants had altered desensitization kinetics. Our study provides the genetic and functional evidence that mutant iGluR3 with altered kinetic properties is associated with moderate cognitive impairment in humans.

glutamate receptor | X-linked mental retardation

Mental retardation (MR) affects 2–3% of the general population (1, 2) and is defined by significant limitations in intellectual function and adaptive behavior that occur before 18 years of age. The etiology for mental retardation is highly heterogeneous, involving many cellular pathways and processes (3, 4). Both genetic defects and environmental insults, alone or in combination, are known to cause cognitive impairment in humans (5, 6). Numerous studies have established that genetic defects likely account for >50% of the identifiable causes of mental retardation (6). X-linked MR (XLMR) occurs in 1 in 600 males and is genetically heterogeneous with an estimated 150–200 responsible loci on the X chromosome (7, 8). Steady progress has been made over the last 15 years with the identification of 59 XLMR genes, primarily by using classical genetic approaches (8). However, with the identification of the relatively common genetic causes for XLMR disorders, the majority of the remaining ≈100 or so XLMR genes are likely found in a small number of families with fewer affected individuals and in patients with less severe cognitive impairment (7–9). These characteristics reduce the effectiveness of classical genetic approaches for identifying the remaining XLMR genes.

L-glutamate is a predominant neurotransmitter that mediates excitatory neurotransmission in CNS via activation of ionotropic and metabotropic receptor families (10–12). The ionotropic glutamate receptor family (iGluRs) consists of three major types: NMDA, α-amino-3-hydroxy-5-methyl-4-isoxazolepropionic acid (AMPA), and kainate, each containing multiple subunits that are assembled into heteromeric functional receptors (12, 13). Key functional domains of these receptors (transmembrane domains, ligand-binding domains, and receptor channel core) have been characterized experimentally (14, 15). Both *in vitro* and *in vivo* animal studies indicated that these receptors are essential for the induction and maintenance of long-term potentiation and long-term depression, two cellular models of learning and memory (16–18). Despite this progress, our understanding on how ionotropic glutamate receptor signaling pathways contribute to human brain development, cognitive function, and diseases remains very limited (8).

In a screen for candidate XLMR genes using an X chromosome cDNA microarray, we identified one proband with an ≈10-fold reduction of *GRIA3* expression (19). Although sequence analysis of *GRIA3*, including all 17 exons plus ≈150 bp of flanking introns and ≈500 bp of proximal promoter in this patient failed to identify a causative variant, this result plus the identification of a complete *GRIA3* deletion in another XLMR patient (see below) led us to sequence *GRIA3* in 400 unrelated XLMR probands. Here, we describe genetic identification, functional characterization, and phenotypic correlation of naturally occurring mutations (one deletion and four missense variants) in key functional domains of iGluR3 in patients with XLMR.

Results

Reduction of *GRIA3* Expression in Males with XLMR. In a screen of lymphoblast RNA from 43 unrelated male XLMR probands, we

Author contributions: Y.W., L.Z., D.V., R.L.H., and T.W. designed research; Y.W., A.C.A., G.R., A.K.S., G.T., T.H., E.S., Y.J., J.R., J.B., P.T., F.L.R., J.N., J.G., and T.W. performed research; A.C.A., G.R., A.K.S., G.T., T.H., L.Z., F.L.R., G.F., M.S., A.F., J.G., R.S., C.E.S., R.L.H., and T.W. contributed new reagents/analytic tools; Y.W., A.C.A., G.R., A.K.S., T.H., G.F., J.G., and T.W. analyzed data; and Y.W., D.V., and T.W. wrote the paper.

The authors declare no conflict of interest.

Abbreviations: AMPA, α-amino-3-hydroxy-5-methyl-4-isoxazolepropionic acid; iGluR, ionotropic AMPA receptors; MR, mental retardation; XLMR, X-linked MR.

[l]To whom correspondence should be addressed. E-mail: twang9@jhmi.edu.

This article contains supporting information online at www.pnas.org/cgi/content/full/0708699104/DC1.

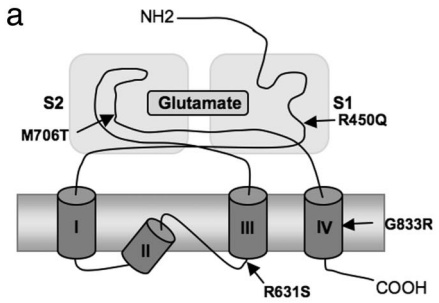

c

Species	Amino Acid Residues			
H. sapiens	R450	R631	M706	G8
P. troglodytes	R	R	M	G
C. familaris	R	R	M	G
M. musculus	R	R	M	G
R. norvegicus	R	R	M	G
G. gallus	R	R	M	G
F. rubripes	R	R	M	G
D. rerio	R	R	M	G

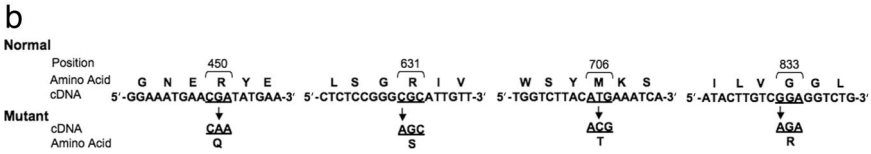

Fig. 1. Location and amino acid conservation of iGluR3 missense variants in males with XLMR. (*a*). Schematic diagram of the location of the four missense variants in iGluR3. (*b*) Sequence annotation of the four missense variants in iGluR3. (*c*) Evolutionary conservation of the amino acids involved.

identified one with a >10-fold reduction in the expression of *GRIA3* (encoding iGluR3) located at Xq25 (19). Quantitative RT-PCR confirmed the reduction of *GRIA3* mRNA, and RT-PCR showed that the residual transcript was of normal size. Southern blot analysis did not reveal any evidence for a genomic rearrangement in or near the *GRIA3* locus (data not shown). We sequenced the PCR products from all 17 *GRIA3* exons plus ≈150 bp of flanking introns, ≈500 bp of the proximal promoter, and ≈2.1 kb of the ultra-conserved region down-stream of the 3′ UTR [supporting information (SI) Table 1] but identified no sequence variant that is likely responsible for the *GRIA3* transcript reduction. In a parallel study using an X chromosome array comparative genomic hybridization (CGH), we identified another proband with a 0.4-Mb deletion at Xq25 (122.00–122.40 Mb) in which *GRIA3* appeared to be the only gene deleted (SI Fig. 7 and *SI Text*). These observations stimulated us to sequence *GRIA3* in an additional 400 unrelated males with MR and a pedigree consistent with X-linked inheritance.

***GRIA3* Missense Variants in Males with XLMR.** We identified four *GRIA3* missense variants (G833R, M706T, R631S, and R450Q), each in a single proband. All four variants are in critical regions of iGluR3: G833R is located within transmembrane domain (TM)-4; M706T is located within the S2 ligand-binding domain (14); R631S is located at the edge of TM3 facing the cytoplasm, 6 aa from the predicted channel core (15); and R450Q is located within the S1 ligand-binding domain (14) (Fig. 1*a*). The residues at all four positions are conserved across vertebrate evolution, including fish (Fig. 1 *b* and *c*). We found none of the variants in a screen of 500 control males. G833R, M706T, and R631S cosegregated with the MR phenotype (Fig. 2 *a*–*c*). R450Q was present in the proband's mother and a maternal uncle who was described by family members as having normal cognitive function but having had no formal IQ testing (Fig. 2*d*). In the respective families, patients with G833R ($n = 2$) have moderate MR, macrocephaly, seizures, myoclonic jerks, and autistic behavior; patients with R631S ($n = 4$) have moderate MR and aesthenic body habitus; patients with M706T ($n = 2$) have mild to moderate MR, aesthenic body habitus, poor muscle bulk, distal muscle weakness, and hyporeflexia. Patients with the 0.4-Mb *GRIA3* deletion ($n = 3$) have moderate MR, reduced muscle bulk, and hyporeflexia.

iGluR3-G833R Reduction Due to Endoplasmic Reticulum Protein Misfolding. We performed *in vitro* functional studies on *GRIA3* missense variants in transiently transfected HEK293 cells. All four produce stable *GRIA3* mRNA (Fig. 3*a*). On immunoblots, iGluR3-M706T, iGluR3-R631S, and iGluR3-R450Q were present in amounts similar to WT iGluR3, (96%, 93%, and 89% of WT, respectively), whereas iGluR3-G833R was present in a substantially reduced amount (22% of WT) (Fig. 3 *b* and *c*).

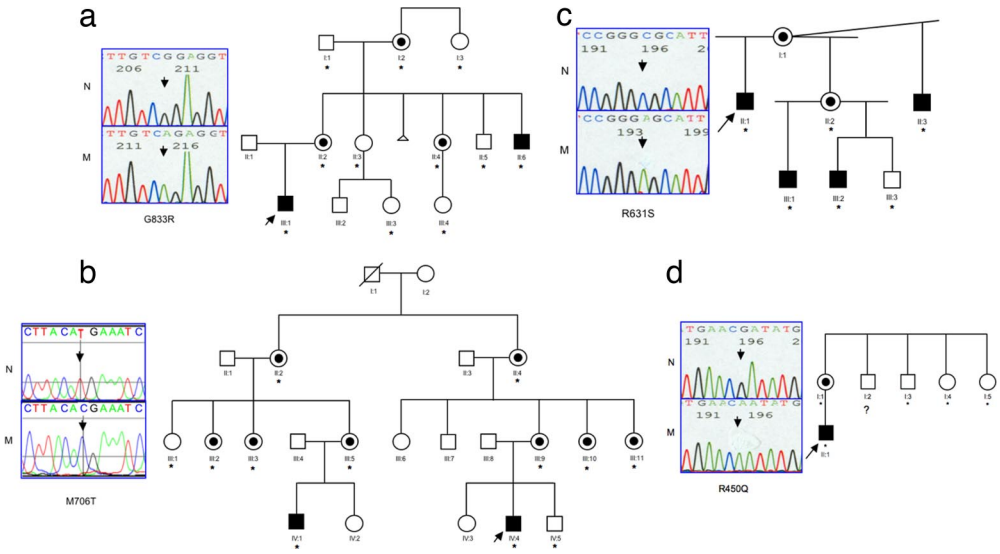

Fig. 2. DNA sequence and pedigrees of four iGluR3 missense variants in the respective proband families. (*a*) G833R. (*b*) M706T. (*c*) R631S. (*d*) R450Q. N, normal; M, mutant. Arrows indicate the probands in the respective families. Filled symbols indicate males with MR; open symbols indicate males or females without MR. Circles with dots indicate obligated female carriers. Asterisks indicate individuals who were genotyped for the indicated *GRIA3* alleles in the respective families and for whom the results were consistent with their clinical phenotype. The question mark in *d* (I-2) indicates the apparent normal maternal uncle who was found positive for the R450Q allele.

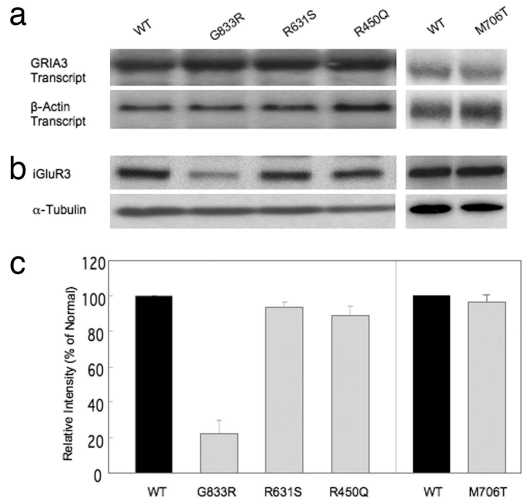

Fig. 3. Northern blot and immunoblot analyses of the iGluR3 missense variants in transfected HEK293T cells. (*a*) Northern blot analysis was done using cDNA probes for human *GRIA3* (nucleotides c.281 to c.1070) and β-actin. Note that there is no significant difference in *GRIA3* transcript levels between WT and the variants. (*b*) Immunoblotting was done using α-iGluR3 (JH4300) and α-β-tubulin antibodies. Note that all four variants generate protein products of comparable size as compared with WT and a substantial reduction of iGluR3-G833R protein. (*c*) Quantification of iGluR3 protein products. Each data point represents mean ± SEM of the relative amount of iGluR3 compared with the WT ($n = 5$). Note that the iGluR3-G883R was ≈22% of the WT-iGluR3.

To understand the molecular mechanism for the reduced amount of iGluR3-G833R, we cultured transiently transfected HEK293 cells expressing either iGluR3-WT or iGluR3-G833R at 30°C for 48 h or at 37°C for 24 h in a medium containing 10 μM lactacystin, a specific 20S proteasome inhibitor (20, 21). We found a 4-fold increase in iGluR3-G833R compared with levels of iGluR3-WT (Fig. 4*a*) in cells cultured at 30°C, and we found a 3-fold

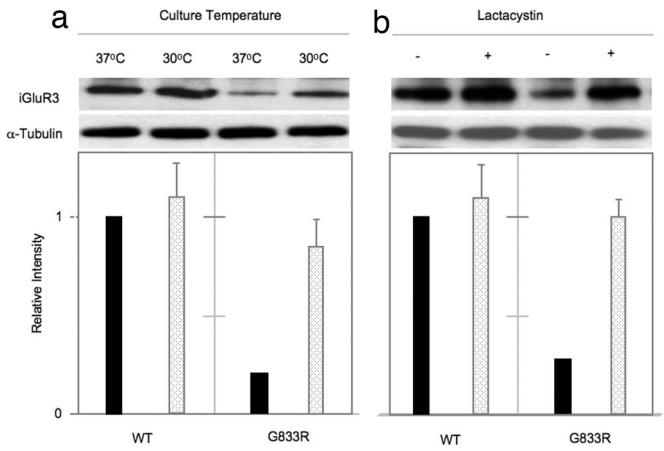

Fig. 4. Protein misfolding studies of the iGluR3-G833R variant. (*a*) HEK293 cells transfected with either WT or iGluR3-G833R expression constructs were cultured at 37°C or 30°C for 48 h. Immunoblot analysis was performed using α-iGluR3 (JH4300) and α-β-tubulin. Note that culturing cells at 30°C restores iGluR3-G833R protein to a near normal level. Each data point represents mean ± SEM of the relative amount of iGluR3 at 30°C compared with that at 37°C ($n = 3$). (*b*) HEK293 cells transfected with either the WT or iGluR3-G833R expression constructs were cultured at 37°C in standard medium for 24 h and then switched to a medium containing lactacystin (10 μM) for another 24 h. Immunoblotting was performed using α-iGluR3 (JH4300) and α-β-tubulin. Note that iGluR3-G833R protein was restored to near normal levels in the culture medium that contained lactacystin. Each data point represents mean ± SEM of the relative amount of iGluR3 in media with or without lactacystin ($n = 3$).

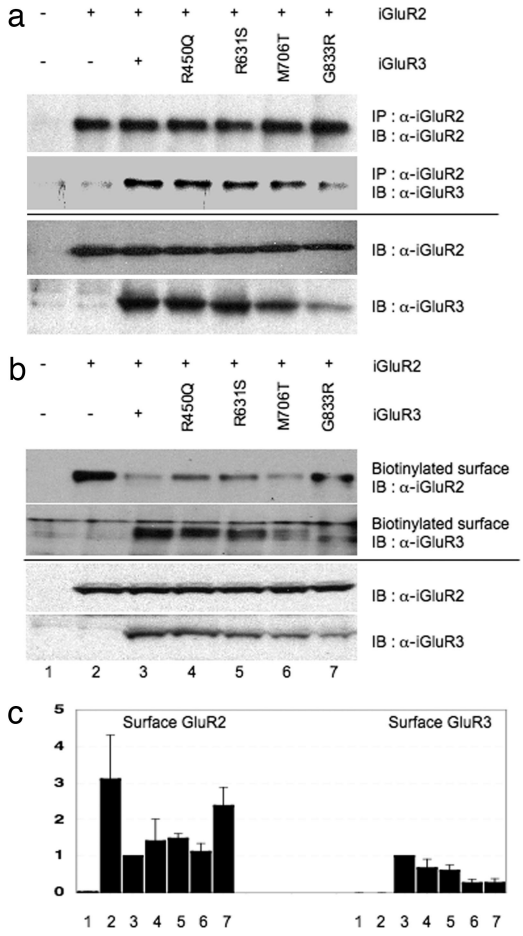

Fig. 5. Levels of plasma membrane expression and effects of the iGluR3 variants on heteromeric assembly with iGluR2. (*a*) Coimmunoprecipitiation of iGluR2 with either the WT or each of the iGluR3 variants in lysates of transfected HEK293T cells. (*Upper*) IP with α-iGluR2 (JH4297) and immunoblotting (IB) with either α-iGluR2 (JH4297) or α-iGluR3 (JH4300) are shown. (*Lower*) The expression of each protein was confirmed by IB using the indicated antibodies. (*b*) Surface expression of the wt-iGluR2/iGluR3 variants in transfected HEK293T cells. (*Upper*) Total membrane proteins from HEK293T cells transfected with expression constructs of WT-iGluR2 and either WT or each of the iGluR3 variants (1:1 ratio) were obtained using a surface biotinylation pull-down method 48 h after transfection and were immunoblotted with either α-iGluR2 (JH4297) or α-iGluR3 (JH4300), respectively. (*Lower*) Expression of each protein product was confirmed by immunoblotting using the indicated antibiotics. (*c*) Each data point represents the mean ± SEM, reflecting the relative abundance of iGluR2 and iGluR3 in the plasma membrane fraction ($n = 3$).

increase in iGluR3-G833R (Fig. 4*b*) in cells cultured in medium containing lactacystin. In both experiments, we were able to restore iGluR3-G833R to near the levels of iGluR3-WT. These results support the hypothesis that the reduction of iGluR3-G833R is likely the result of rapid degradation of an abnormally folded receptor protein involving proteosome.

Effects of iGluR Missense Variants on Heteromeric iGluR2/3 Assembly. The endogenous AMPA receptors consist of primarily either iGluR2/3 or iGluR1/2 heteromers (12, 13). To evaluate the influence of these iGluR3 variants on the assembly of heteromeric iGluR2/3 receptors, we first conducted coimmunoprecipitation using HEK293 cells cotransfected with expression constructs for WT-iGluR2 and each of the four iGluR3 variants (1:1 ratio) (Fig. 5*a*). When the IP was done with α-iGluR2, we observed the expected reduced amount for iGluR3-G833R but no substantial difference for the other three variants (R450Q, R631S, and M706T)

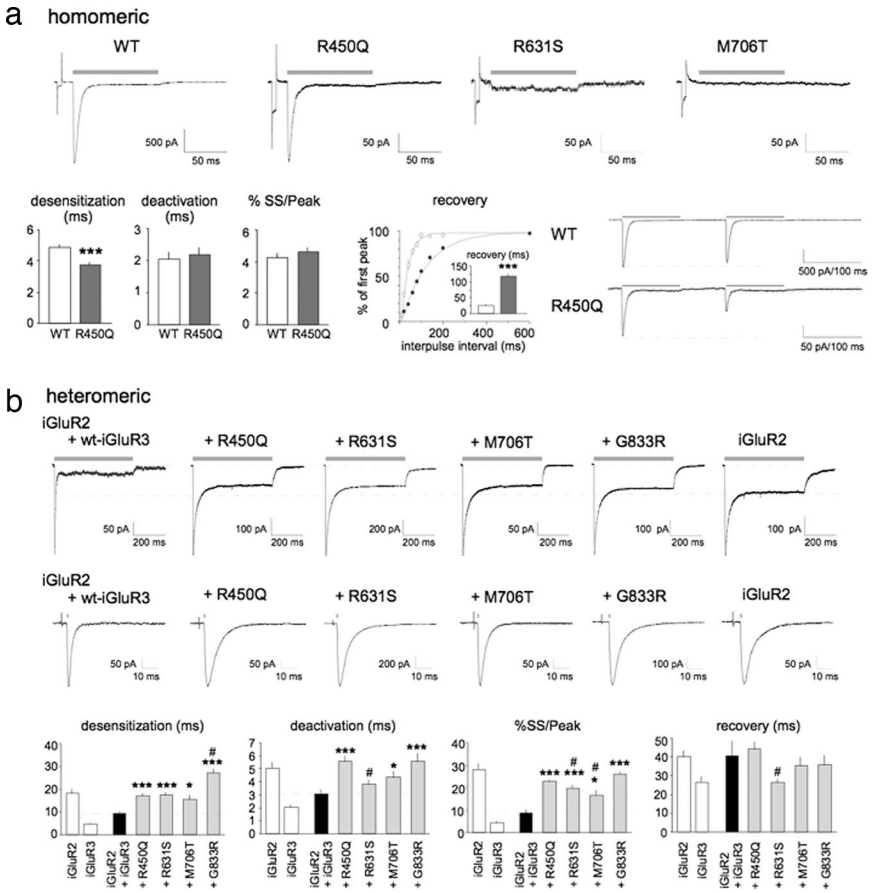

Fig. 6. Electrophysiological properties of iGluR3 variants in homomeric and heteromeric receptors. A whole-cell voltage-clamp recording was made from HEK293 cells 48–72 h after transfection. After establishing whole-cell contact, the cell was lifted and positioned in a constant stream of recording solution. Long or short pulses of 10 mM glutamate were applied using a piezo-driven fast solution switch system (see *Methods*). The holding potential was −70 mV. Summary data are shown as the mean and SEM, and Student's *t* test (two-tailed) was used for statistical analysis. (*a*) Glutamate-induced currents produced by homomeric iGluR3 receptors. (*Upper*) Representative traces for WT and each of the iGluR3 variants; glutamate was applied for 100 ms as indicated by the horizontal bar. (*Lower*) Comparison of kinetic properties for WT-iGluR3 (WT, $n = 7$) and iGluR3-R450Q ($n = 9$–10). ''% SS/Peak'' denotes the percentage of the steady-state current relative to the peak current. ***, $P = 0.001$. Recovery from desensitization (''recovery'') was measured by applying two 100-ms pulses at different intervals. The peak amplitude of the second response relative to the first (percent of first peak) was plotted against the interpulse interval (WT, $n = 4$; R450Q, $n = 6$). Recovery time constants were calculated by fitting the data with a single exponential function. (*Inset*) (*Left*) Averaged data are given. (*Right*) Representative traces with an 80-ms interval are shown. ***, $P < 0.001$. (*b*) Glutamate-induced currents of iGluR receptors formed when coexpressing iGluR3 variants with WT-iGluR2. Representative traces are shown for 500 ms (*Top*) and 1 ms pulses (*Middle*) of 10 mM glutamate. The traces on the far right are from homomeric WT-iGluR2 receptors. The bar graphs show summary data from 9 (+WT-iGluR3), 5 (+R450Q), 7–8 (+R631S), 11(+M706T), and 4 (+G833R) experiments. For comparison, data have been included for homomeric iGluR2 ($n = 8$) and WT-iGluR3 ($n = 7$). *, $P < 0.05$; ***, $P < 0.005$ vs. WT-iGluR2/3; #, $P < 0.05$, mutant heteromers vs. homomeric iGluR2. Recovery time constants were measured in three or four experiments.

from WT. We then used a biotin-mediated cell membrane protein pull-down method to determine the relative abundance of iGluR2 and each of the iGluR3 variants in the plasma membrane fraction (Fig. 5*b*). Compared with the WT-iGluR3, we found no significant difference for iGluR3-R450Q and iGluR3-R631S, but we did find a substantial reduction for iGluR3-G833R and iGluR3-M706T (>2-fold) (Fig. 5*c*).

Homomeric iGluR3 Variants Are Associated with Altered Channel Function. To evaluate the effects of these iGluR3 variants on the electrophysiological properties of AMPA receptors, we conducted whole-cell recording studies on HEK293 cells transfected with expression constructs of WT and each of the variants (Fig. 6*a*). Homomeric iGluR3-R450Q produced currents with desensitization and deactivation time constants similar to those of WT receptors. However, desensitization was slightly accelerated, and recovery from desensitization was drastically slowed (117 ± 10 ms vs. 26 ± 3 ms; $P < 0.01$). Homomeric iGluR3-R631S and iGluR3-M706T produced minimal or no current, suggesting that these subunits, when expressed alone, are not effectively trafficked to the surface or do not form a functional receptor.

Heteromeric iGluR2-wt/iGluR3 Variants Show Distinct Channel Kinetic Properties. To investigate the functional consequences of iGluR3 variants as iGluR2/3 heteromers, we conducted whole-cell recording studies on HEK293 cells cotransfected with iGluR2-WT and each of the iGluR3 variants (1:1 ratio). The iGluR2-WT and iGluR3-WT homomers demonstrated highly distinct kinetics properties in that the latter has 3- to 4-fold faster desensitization and deactivation and 8-fold smaller steady-state/peak ratios (Fig. 6*b*). The iGluR2/3-WT heteromers exhibited kinetic properties intermediate between those of the homomers. When iGluR2-WT was coexpressed with each iGluR3 variant, the responses were significantly different from those of the WT heteromers (Fig. 6*b*). Desensitization time constants for these variants were 1.5- to 3-fold larger than that of the WT heteromers and were comparable to that of the GluR2-WT homomers. Similarly, steady-state/peak ratios for iGluR3-R450Q or iGluR3-G833R were significantly higher than

that of the WT heteromers and were comparable to the iGluR2-WT homomers. Interestingly, the steady-state/peak ratios for iGluR3-R631S and iGluR3-M706T were intermediate between the WT heteromer and iGluR2 homomer but were statistically different from both. This data suggests that R631S and M706T are incorporated into the heteromeric receptors but perhaps with altered stoichiometry or a reduced impact on overall kinetic properties. There is little evidence that either the iGluR-R450Q or iGluR3-G833R variants are present in a substantial number in heteromeric receptors, because most kinetic parameters were indistinguishable from those of WT-iGluR2 homomers (Fig. 6*b*).

Discussion

AMPA receptors mediate fast excitatory synaptic transmission in the CNS and are crucial to brain development and activity-dependent synaptic plasticity (12, 13). AMPA receptor modulators that alter receptor kinetics may influence long-term potentiation, long-term depression (22–24), and various forms of memory function in both animals (23, 25, 26) and humans (27, 28). Mice with either a *GRIA1* or *GRIA3* gene deletion showed significant changes in hippocampal long-term potentiation (18, 29). A female with moderate MR, seizures, and bipolar disorder was found to have an apparently balanced chromosomal translocation t(X;12)(q24;q15) that interrupted *GRIA3* (30).

We identified a complete genomic deletion and four missense variants in *GRIA3* involving highly conserved residues in key functional domains of iGluR3, including one missense variant (G833R) that is associated with a 78% reduction of receptor protein and two missense mutations (M706T and R631S) that are associated with minimal or no channel current on whole-cell recording, in multiple affected individuals in the respected XLMR families. These mutations cosegregated with MR phenotype in the proband families and were found to be absent in 600 normal males. In two families (iGluR3-R631S and iGluR3-M706T), linkage-analysis data were consistent with the primary disease loci at Xq25. In three families (iGluR3-G833R, iGluR3-M706T, and iGluR3-R450Q), sequence analysis was conducted on 737 vertebrate genome annotation (VEGA)-annotated X chromosome genes, including all known XLMR genes, and no obvious disease causing mutations in these genes were found. Interestingly, these mutants with an apparent loss of iGluR3 function due to gene deletion, reduced receptor protein, or loss of channel current share similar a clinical phenotype: moderate MR, poor muscle bulk, muscle weakness, asthetic body habitus, and hyporeflexia.

Because the native AMPA-type of glutamate receptors consists of heteromeric GluR1/2 and GluR2/3, there are several possible reasons why there is a lack of significant contribution of the iGluR3 mutants to the overall channel kinetic properties of the heteromers: (*i*) a reduced total amount of mutant iGluR3 subunit on plasma membrane due to either protein instability (G833R) or a potential-membrane trafficking defect (M706T); (*ii*) a nonfunctioning iGluR3 subunit as suggested by minimal or no channel current recorded for both iGluR3-R631S and iGluR3-M706T homomers; or (*iii*) defects in GluR2/3 heteromeric assembly due to these mutants. Data from the current studies could not distinguish these mechanisms but do suggest that there is a lack of significant contribution of the iGluR3 mutants into functional iGluR2/3 heteromer. These data support the conclusion that missense variants (M706T, G833R, and R631S) are associated with significant defects of iGluR3 function. iGluR3-R450Q produces a stable receptor protein, normal membrane trafficking, and normal currents on whole-cell recording but with distinct kinetic changes in that desensitization was slightly accelerated and recovery from desensitization was drastically slowed. Because this variant was also found in a male with apparent normal cognitive function, it is not clear from the current study how these kinetic alterations relate to the MR phenotype.

Our studies provide genetic and functional evidence that mutations in functional domains of iGluR3 produce kinetic changes in AMPA receptor function and that a significantly reduced iGluR3 channel function is associated with moderate MR and a distinct neurological phenotype in humans. Although it is tempting to speculate that the kinetic alterations of these mutants directly contribute to MR, their effects may be indirect through changing neuronal development or altering neuronal circuits. Studying animal models that express these mutant receptors should provide a system to examine how mutations in iGluR3 contribute to cognitive impairment in humans.

Materials and Methods

Samples. Males with MR and a pedigree consistent with X-linkage were recruited from patients followed at Greenwood Genetic Center (Greenwood, SC) and the Johns Hopkins Hospital (Baltimore, MD). The human subject research protocols were approved by the Institutional Review Board at both institutions. An informed consent was obtained from each study patient and/or their parents or guardians. These patients were evaluated by clinical geneticists and underwent standard laboratory evaluations for mental retardation. All patients had a normal karyotype and a negative molecular test for fragile X syndrome, as well as a negative screen for common inborn errors of metabolism. For each patient, 5–10 ml of blood was collected to establish lymphoblast cell lines by Epstein–Barr virus transformation. Cell lines and DNA samples from additional XLMR patients, and normal controls were obtained from Greenwood Genetic Center, Coriell Cell Repositories (Camden, NJ), ECACC (Salisbury, U.K.), and a cohort of samples from males with XLMR collected for the Genetics of Learning Disability (GOLD) Study (Cambridge, U.K.), with appropriate U.K. Medical Research Educational Centre approval. This cohort includes samples from New South Wales, Australia; Greenwood, SC; and the U.K. Among the 400 XLMR families enrolled in the study, ≈20% have linkage analysis data (LOD >2.0) for the responsible loci on the X chromosome, including the families with *iGluR3*-R631S and *iGluR3*-M706T; ≈62% (250 of 400) of the probands were sequenced for 737 vertebrate genome annotation (VEGA)-annotated X chromosome genes that include all known XLMR genes. The study identified no obvious disease-causing mutations in these genes in the probands with *iGluR3*-G833R, *iGluR3*-M706T, and *iGluR3*-R450Q (31, 32).

Mutation Analysis. Genomic DNA was extracted from lymphoblast cell lines. For each sample, 17 exons of *GRIA3* (NM007325, flip; NM000228, flop) with 150-bp flanking introns were PCR-amplified using HotMaster TaqDNA polymerase (Eppendorf, Boulder, CO) according to the manufacturer's instruction. PCR amplicons and primer sequences are provided in SI Table 1. PCR products were purified by Exo1/SAP following a standard protocol (Applied Biosystems, Foster City, CA). Sequencing was performed using ABI PRISM BigDye Terminator Cycle Sequencing kit on an ABI3100 automatic DNA sequencer (Applied Biosystems).

Expression Constructs. The full-length *GRIA3* cDNA was cloned into pcDNA3 vector (Invitrogen, Carlsbad, CA) between EcoRV and NotI sites. The flip form iGluR3 with unedited A at the R/G editing site was used for subsequent experiments. The full-length *GRIA2* cDNA was cloned in the pRK5 expression construct. The iGluR3 variants (G833R, M706T, R631S, and R450Q) were generated using the QuikChange site-directed mutagenesis kit (Stratagene, La Jolla, CA) according to the manufacturer's instructions.

Cell Culture and Transfection. HEK293T cells have no detectable endogenous *GRIA3* expression, serve as a clean system to study exogenous expression from *GRIA3* vectors, and are standard cells for electrophysiological recording studies of channel kinetics of glutamate receptors (24). The cells were cultured in DMEM

supplemented with 10% FBS, 100 units/ml penicillin, and 100 mg/ml streptomycin at 37°C in 5% CO_2. The culture medium was replenished every 3 days. Transient transfection was conducted using either FuGENE6 or calcium phosphate methods according to the manufacturer's instruction (Roche, Indianapolis, IN).

Northern Blot Analysis. Total RNA was isolated from transfected HEK293T cells by using TRIzol reagent (Invitrogen). Northern blot analysis was conducted according to a standard protocol (33) by using a ^{32}P-labeled human GRIA3-cDNA probe (789 bp, nucleotides c.281 to c.1070) and a cDNA probe for β-actin (Ambion, Austin, TX).

Immunoblotting. Transfected HEK293T cells were harvested in a lysis buffer containing 1% TritonX-100 and protease inhibitor mixture (Roche). Protein concentration was determined using a BCA protein assay kit (Pierce, Rockford, IL). Twenty μg of protein was resolved using SDS/7.5% PAGE and was transferred to a nitrocellulose membrane. The blot was blocked using 5% nonfat milk in 1x Tris-buffered saline Tween-20 (TBST) at room temperature for 1 h and then incubated in respective primary polyclonal antibodies, α-GluR3 (JH4300) or α-GluR2 (JH4297), overnight at 4°C. After washing, the blot was incubated in respective HRP-labeled secondary antibody (PerkinElmer, Boston, MA) at RT for 1 h. The target proteins were visualized using an ECL kit (Pierce) according to the manufacturer's instruction. The intensity of the target protein bands was quantified using ImageQuant 5.2 software (Molecular Dynamics, Sunnyvale, CA).

Coimmunoprecipitation. HEK293T cells were transfected with the described combinations of pRK5-GluR2 and the WT or variants of pcDNA3-GRIA3 (iGluR3) (5 μg:5 μg) by using a standard calcium phosphate method. At 48 h after transfection, the cells were lysed in TNE buffer containing 50 mM Tris·HCl (pH8.0), 150 mM NaCl, 20 mM EDTA, 1% Triton X-100, 10 μg/ml aprotinin, and 10 μg/ml leupeptin, and were immunoprecipitated with an α-GluR2 (JH4297) antibody. Immunoprecipitated samples and total cell lysates were resolved using SDS/PAGE followed by immunoblotting using either α-GluR2 (JH4297) or α-GluR3 (JH4300).

Cell-Surface Protein Biotinylation and Pull-Down. HEK293T cells transiently transfected with expression constructs of the described combination were cooled on ice 48 h after transfection, washed twice with ice-cold PBS containing 5 mM $MgCl_2$ and 1 mM $CaCl_2$, and then incubated in PBS containing 5 mM $MgCl_2$, 1 mM $CaCl_2$, and 1 mg/ml Sulfo-NHS-SS-Biotin (a membrane-impermeable derivative of biotin) for 20 min on ice according to the instructions provided in the Protein Biotinylation and Purification kit (Pierce). Unreacted biotinylation reagent was removed using a quench buffer and was washed three times with ice-cold TBS [50 mM Tris·HCl (pH 7.5), 150 mM NaCl]. The cells were harvested in RIPA buffer containing 10 mM Tris·HCl (pH 7.5), 150 mM NaCl, 1 mM EDTA, 1% Triton X-100, 0.1% SDS, 0.1% sodium deoxycholate, 10 μg/ml aprotinin, and 10 μg/ml leupeptin. The cell homogenates were centrifuged at 15,000 $\times$ g for 20 min at 4°C. The resulting supernatant was incubated with NeutrAvidin beads (Pierce) for 3 h at 4°C. The biotinylated proteins were resolved on SDS/PAGE followed by immunoblotting using respective antibodies.

Whole-Cell Recording from HEK293 Cells. HEK293 cells were transfected with plasmids for iGluR3 variants either alone or in combination with pRK5-iGluR2 (1:1 ratio) by using lipofectamine 2000 (Invitrogen CA). A plasmid expressing eGFP was routinely included in the transfection mixture at 1/20th of total DNA for visualization during recording. Transfected cells were maintained at 36.5°C in MEM (Invitrogen) supplemented with 10% newborn calf serum (Sigma, St. Louis MO), penicillin/streptomycin and 100 μM DNQX (Sigma). One day before recording, the cells were transferred to a coverglass coated with polyD-lysine (0.1 mg/ml). Experiments were typically carried out 48–72 h after transfection.

A whole cell voltage-clamp recording was made with a glass pipette (2–5 megohms) containing 130 mM CsF, 10 mM EGTA-K, 2 mM ATP-Mg, 0.1 mM spermine, and 10 mM Hepes (pH 7.3). After establishing whole-cell contact, cells were lifted and positioned in a constant flow of the recording solution containing 140 mM NaCl, 3 mM KCl, 2 mM $CaCl_2$, 1 mM $MgCl_2$, 5 mM glucose, 10 mM and Hepes (pH 7.3). A pulse of glutamate (10 mM) was applied to the cell by rapidly moving the solution application pipette with a piezo translator. Responses were recorded with Axo-Patch-1D (Axon Instruments, Union City, CA) at a filter frequency of 5 kHz, and the signals were digitized at 10 kHz by using Digidata 1322A/ pClamp 8 (Axon Instruments). The holding potential was -70 mV, and all of the experiments were carried out at ambient temperature (24 $\pm$ 1°C)

Typically, 10 consecutive responses were averaged for further analysis. The desensitization and deactivation time constant was calculated by fitting the decay phase of the response with a single exponential function. Responses with a rise time slower than 0.8 ms and a peak amplitude $<$100 pA were excluded from analysis. All of the results are expressed as mean and SEM, and Student's t test (two-tailed) was used for statistical analysis.

We thank Ms. Marie Shaw for technical assistance. This work was supported in part by National Institute of Child Health and Human Development Grants HD044789 (to T.W.) and HD26202 (to C.E.S.); the Basil O'Connor Award from the March of Dimes Foundation (to T.W.); the Passano Physician Scientist Award (to T.W.); a grant from the South Carolina Department of Disabilities and Special Needs (to C.E.S.); National Institute of Child Health and Human Development Mental Retardation Research Centers Grant HD24061; National Institute of Neurological Disorders and Stroke Grants NS41020 (to A.C.A.) and NS36715 (to R.H.); National Health and Medical Research Council (Australia) Program Grant 400121 (to J.G.); and the Wellcome Trust (United Kingdom). R.H. is an Investigator with the Howard Hughes Medical Institute.

1. McLaren J, Bryson S (1987) *Am J Ment Retard* 92:243–254.
2. Crow Y, Tolmie J (1998) *J Med Genet* 35:177–182.
3. Johnston M (2003) *Eur J Paediatr Neurol* 7:105–113.
4. Chelly J, Mandel J (2001) *Nat Rev Genet* 2:669–680.
5. McQueen P, Spence M, Garner J, Pereira L, Winsor E (1987) *Am J Ment Defic* 91:460–466.
6. Stevenson R, Procopio-Allen A, Schroer R, Collins J (2003) *Am J Med Genet* 123:29–32.
7. Stevenson R (2005) *Curr Opin Pediatr* 17:720–724.
8. Ropers H, Hamel B (2005) *Nat Rev Genet* 6:46–57.
9. Stevenson R, Schwartz C (2002) *Cytogenet Cell Genet* 99:265–275.
10. Seeburg P (1993) *Trends Neurosci* 16:359–365.
11. Hollmann M, Heinemann S (1994) *Annu Rev Neurosci* 17:31–108.
12. Mayer M, Armstrong N (2004) *Annu Rev Physiol* 66:161–181.
13. Simeone T, Sanchez R, Rho J (2004) *J Child Neurol* 19:343–360.
14. Kuusinen A, Arvola M, Keinanen K (1995) *EMBO J* 14:6327–6332.
15. Wo Z, Oswald R (1995) *Trends Neurosci* 18:161–168.
16. Bliss T, Collingridge G (1993) *Nature* 361:31–39.
17. Bredt D, Nicoll R (2003) *Neuron* 40:361–379.
18. Zamanillo D, Sprengel R, Hvalby O, Jensen V, Burnashev N, Rozov A, Kaiser K, Koster H, Borchardt T, Worley P, *et al.* (1999) *Science* 284:1805–1811.
19. Zhang L, Jie C, Obie C, Abidi F, Schwartz C, Stevenson R, Valle D, Wang T (2007) *Genome Res* 17:641–648.
20. Denning G, Anderson M, Amara J, Marshall J, Smith A, Welsh M (1992) *Nature* 358:761–764.
21. Fenteany G, Standaert R, Lane W, Choi S, Corey E, Schreiber S (1995) *Science* 268:726–731.
22. Arai A, Lynch G (1992) *Brain Res* 598:173–184.
23. Staubli U, Perez Y, Xu F, Rogers G, Ingvar M, Stone-Elander S, Lynch G (1994) *Proc Natl Acad Sci USA* 91:11158–11162.
24. Arai A, Xia Y, Suzuki E (2004) *Neuroscience* 123:1011–1024.
25. Larson J, Lieu T, Petchpradub V, LeDuc B, Ngo H, Rogers G, Lynch G (1995) *J Neurosci* 15:8023–8030.
26. Hampson R, Rogers G, Lynch G, Deadwyler S (1998) *J Neurosci* 18:2748–2763.
27. Lynch G, Granger R, Ambros-Ingerson J, Davis C, Kessler M, Schehr R (1997) *Exp Neurol* 145:89–92.
28. Ingvar M, Ambros-Ingerson J, Davis M, Granger R, Kessler M, Rogers G, Schehr R, Lynch G (1997) *Exp Neurol* 146:553–559.
29. Meng Y, Zhang Y, Jia Z (2003) *Neuron* 39:163–176.
30. Gecz J, Barnett S, Liu J, Hollway G, Donnelly A, Eyre H, Eshkevari H, Baltazar R, Grunn A, Nagaraja R, *et al.* (1999) *Genomics* 62:356–368.
31. Tarpey P, Raymond, F, O'Meara S, Edkins S, Teague J, Butler A, Dicks E, Stevens C, Tofts C, Avis T, *et al.* (2007) *Am J Hum Genet* 80:345–352.
32. Raymond F, Tarpey P, Edkns S, Tofts, C., O'Meara S, Teague J, Butler A, Stevens C, Barthorpe S, Buck G, *et al.* (2007) *Am J Hum Genet* 80:982–987.
33. Sambrook J, Russel DW, eds (2000) *Molecular Cloning: A Laboratory Manual* (Cold Spring Harbor Lab Press, Cold Spring Harbor, NY), 3rd Ed, pp 7.42–7.45.